EUROGRAPHICS Workshop on Graphics and Cultural Heritage (2018)
R. Sablatnig and M. Wimmer (Editors)

Short Paper

An Investigation of Optimal Light Source Setups for Photometric Stereo Reconstruction of Historical Coins

S. Brenner, S. Zambanini and R. Sablatnig

Computer Vision Lab, Institute of Visual Computing & Human-Centered Technology, TU Wien

Abstract

In this paper, we address the 3D reconstruction of historical coins by means of Photometric Stereo. We investigate the influence of the number and arrangement of lights to the reconstruction quality by comparing mean angular errors on 22 historical coin models. Our results demonstrate that 6 lights circularly placed at an optimal elevation angle do not show a significant loss of reconstruction quality compared to a full semispherical dome setup with 54 lights. This represents a considerable saving of acquisition time and system complexity when it comes to the mass digitization of historical coins.

CCS Concepts

•***Computing methodologies*** → *3D imaging; Reconstruction; Shape inference;*

1. Introduction

Historical coins are fundamental objects of Numismatic research and as such their digitization is of central importance [JHMZF11]. However, the number of coin artifacts present in museum collections can be in the order of hundred thousands: for instance, in the *Coin Cabinet* of the *Vienna Museum of Fine Arts* 600.000 monetary objects are present [KGM]. Like for other heritage artifacts, historical coin mass digitization is a matter of cost-benefit ratio. For this reason, if at all, coins are prevalently captured with 2D photography for digital archiving. However, traditional 2D photography does not account for the actual 3D nature of coins and thus leads to a serious information loss. This loss is not only unfavorable for the documentation but also for the manual and automatic analysis of coins, including their identification and metric measurement [ZSKM09].

For this reason, various acquisition methods beyond traditional 2D photography have been proposed for historical coins. The initial work for an improved visualization of coins is represented by Mudge et al. [MVSL05], who applied Polynomial Texture Mapping (PTM) [MGW01] to medieval coins. PTM, as a special type of Reflection Transformation Imaging (RTI), allows a richer documentation of historical coins as relief details can be visualized by means of an interactive viewer software with a movable virtual light source. RTI was also used to provide an interactive display of ancient coins for visitors at the National Museum of San Matteo in Pisa [PSP*14]. Structured light scanning for historical coins was proposed and evaluated by Hödlmoser et al. [HZKS13]. In their study, 14 ancient and 8 medieval coins were scanned and the resulting 3D models were evaluated w.r.t. volume and diameter measurements on the actual coins. Their results demonstrate the strong low-frequency reconstruction capability of structured light scanning for this kind of objects. MacDonald et al. [MMH17] described a framework for ancient coin reconstruction that combines high frequencies from PS with low frequencies produced by a laser scanner, thus exploiting the strengths of both approaches.

In this paper, we investigate the usage of Photometric Stereo (PS) [Woo80] as a 3D reconstruction method for historical coins. PS is of particular interest in the context of mass digitization of coin collections as it offers an accurate reconstruction of high-frequency surface details with a relatively cheap acquisition setup: in contrast to the more complex hardware setup of structured light approaches, which also have proven to be highly sufficient for coins [NRDR05, HZKS13, MMH17], only a traditional photo camera and a set of distributed light sources are needed. The uncalibrated PS variant [QLD15] provides a further simplification of the digitization process as it eliminates the need for special calibration objects and additional preprocessing steps. For our purpose, we specifically study the influence of the number and placement of the light sources as the chosen setup has a direct impact on the accuracy of the derived 3D reconstructions as well as the effort and time it takes to capture a single coin specimen. In this sense, our work can also be regarded as a guideline for practitioners who aim to digitize large collections of historical coins in 3D.

2. Uncalibrated Photometric Stereo

Photometric Stereo (PS) refers to the reconstruction of depth from a set of images taken under a constant viewpoint and varying lighting directions. The pixel intensities measured in different images are used to estimate surface orientation (normal vectors) and, in an optional second processing step, relative depth. Compared to other vision-based 3D reconstruction approaches, such as active

DOI: 10.2312/gch.20181362

and passive triangulation, the strength of PS lies in the recovery of high-frequency surface details, while it is prone to low-frequency biases [HW11]. This makes PS a promising approach for the acquisition of almost planar cultural heritage objects such as coins, where the recovery of fine details is more important than the global geometry (which is near to planar anyway). Coins exhibit another property that makes them favorable for PS reconstructions: inherent to their production through stamping, they are free from depth discontinuities, which prove to be problematic for PS. These properties manifest in the fact that coins are frequently used as test objects for PS approaches [QMD16, PF13].

Traditional PS assumes that the direction of incident light is known for each image [Woo80]. In practice, this assumption only holds for laboratory setups. Several approaches for the light source calibration have been proposed [AG15], but they mostly rely on special calibration objects and require additional preprocessing steps.

Uncalibrated Photometric Stereo (UPS) subsumes a set of methods that simultaneously estimate surface normals and light directions. Belhumeur et al. [BKY99] showed that under the assumption of an orthogonal projection (which is made across the majority of PS literature) and without further restrictions this problem is ill-posed and can only be solved up to Generalized Bas-Relief (GBR) transformations $\overline{f}(x,y) = \lambda f(x,y) + \mu x + \nu y$, where $f(x,y)$ denotes the height at position (x,y). Approaches to estimate the parameters λ, μ and ν of the GBR transformation rely on regularity measures. Alldrin et al. [AMK07] propose the minimization of the entropy of the albedo map. Queau et al. [QLD15], similarly, employ the total variation of the resulting normal- or depth field as a regularity measure. In contrast to the former approach, it takes spatial relations into account.

Another simplification that is made in PS approaches is the assumption of a purely diffuse material, which never holds for real materials, especially not for coins. While some approaches tackle this problem with more complex reflectivity models [NIK90, AWL13], another more universal approach is to remove outliers of the assumed model (e.g. the diffuse one) from the input data as a preprocessing step. Wu et al. [WGS*10] provide a method to remove shadows and specularities from the input data by low-rank matrix recovery.

3. Experiments

We conducted a series of experiments to evaluate the influence of the number and spatial distribution of light directions on the UPS reconstruction of ancient coins. In the following we describe the image acquisition setup, the employed reconstruction algorithms and our experimental result.

3.1. Input images

For illumination we used an approximately semispherical dome construction with a radius of 45cm, equipped with 54 high-power LEDs. The lights are arranged in 5 horizontal circles with twelve lights on the lower four circles and six lights on the top one. See Figure 1 for illustration.

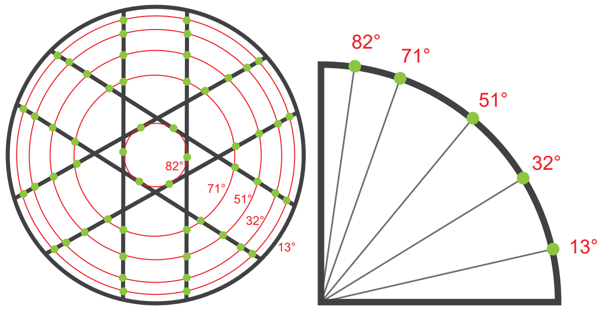

(a) top view (b) side view

Figure 1: Schematic of light dome. Light positions are shown in green.

Our test objects were 11 ancient coins from the Roman Empire, made from brass, copper, silver, gold or billon and showing various degrees of corrosion. Their diameters range between 19 and 33 mm. Each coin was imaged from both sides, leaving us with 22 data sets.

For each light of the dome, an achromatic image was taken from a vertical distance of 60cm with a focal length of 120mm. With that setup, the object surface was sampled with 45 pixels per mm.

3.2. Processing

To remove specularities and shadows from the input data, the preprocessing scheme proposed by Wu et al. [WGS*10] was applied. For surface reconstruction the UPS method proposed by Queau et al. [QLD15] was used, where the total variation of the height field is minimized. The referenced paper describes how the estimation of the simple bas-relief transformation parameter λ may fail if the assumption of constant light magnitude does not hold, leading to a complex value for λ. As this was the case with our test data, we resorted to estimating λ by minimizing the entropy of the albedo map. For objects with regular albedos this is a feasible alternative [QLD15]. The employed method assumes an orthographic projection and parallel lighting, which is a reasonable approximation given the size of the observed objects versus the radius of our light dome [FSB04, LWYG07, ASSS14].

3.3. Results

The objective of this paper is to evaluate the performance of PS reconstruction when using only subsets of the available light directions and comparing the results to the "full dome" reconstruction. As an error metric we use the mean angular error (MAE) of the surface normals, which is common in PS literature [AG15, QLD15]. The following configurations were considered:

3.3.1. Random dropout

Reconstruction is performed with $n \in \{3, 8, \ldots, 53\}$ randomly selected light directions, to test the general assumption that reconstruction quality increases with the number of light directions. For each dataset, the reconstruction test was performed three times per light count, leading to 66 measurements per light count. Figure 2 shows the MAEs averaged across all measurements. Note that

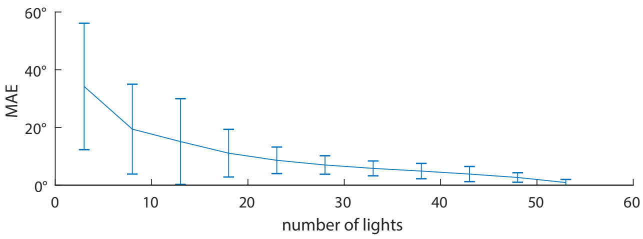

Figure 2: MAE of reconstruction over the number of randomly selected light directions. Vertical bars show the standard deviations.

		number of lights				
		3	4	6	12	mean
elevations	13°	19.3	22.2	17.1	17.5	19.0
	32°	16.1	14.4	14.6	14.5	14.9
	51°	15.0	12.4	10.3	**8.5**	**11.6**
	71°	22.9	19.0	13.8	11.5	16.8
	82°	24.5		26.8		25.7
mean 13°-71°		18.3	17.0	14.0	**13.0**	

Table 1: MAE for elevation angles and number of active lights. Best results are printed bold. Elevation angles are approximated, as the light dome is not calibrated.

while the mean error decreases with an increasing number of lights, also the standard deviation decreases. This leads to the assumption that for constellations with a low number of lights, their positioning has a large impact on the results. Motivated by that, the following experiments aim at investigating optimal configurations for setups using a lower number of lights.

3.3.2. Single elevation

In this experiment, 3, 4, 6 and 12 rotationally symmetric light positions on circles of equal elevation are considered. The goal is to evaluate the substitution of a light dome with a circular light arrangement, and which elevation angle would be preferable for such a setup. Table 1 shows the mean errors across all datasets. The light configuration with 82° elevation angle (close to the camera) shows by far the worst performance. This is justified by the fact that the reconstruction problem becomes ill-conditioned if light directions are too similar [AG15]. On the other hand, in the 13° images a high amount of shadowed areas may lead to bad results. The best results were achieved by a medium elevation of 51°. Like in the previous experiment, the error generally decreases with the number of light directions, however, some elevations show slight deviations from that tendency.

Comparing this experiment to the previous one, it can be concluded that a circular symmetric light arrangement can significantly reduce the number of necessary lights in comparison to lights randomly distributed over a hemisphere, if it is placed at an optimal angle of elevation. For example, 6 lights at 51° show an MAE of 10.3. In the random dropout experiment, this error is undercut only with 23 active lights.

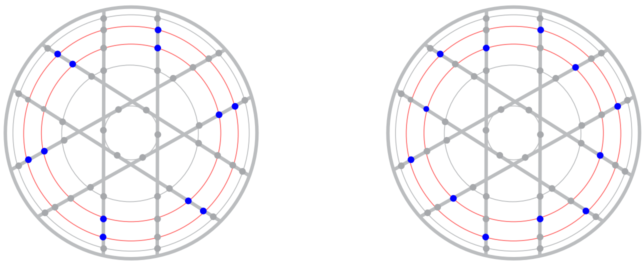

(a) aligned (b) twisted

Figure 3: Example of the aligned and twisted configuration of six lights per elevation. Active light positions are shown in blue.

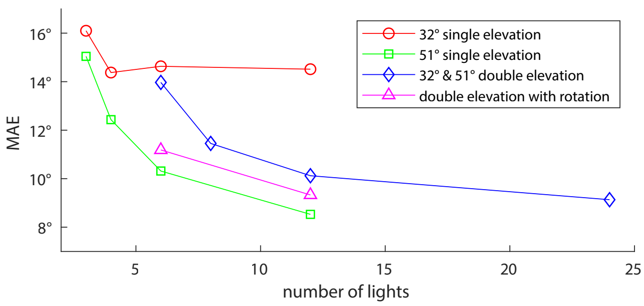

Figure 4: Errors for two single elevations and their combinations. The x-axis refers to the total number of active lights.

3.3.3. Double elevation

The two best performing elevations from the previous experiment (32° and 51°) are used to observe the effect of distributing a number of light directions across two circles of elevation instead of one. We used the same light azimuths as in the previous experiment, but on two elevation angles simultaneously. Additional tests were made for the three- and six-lights settings, with the active lights on the upper circle twisted to a complementary configuration, as illustrated in Figure 3.

The results shown in Figure 4 can be interpreted as follows. Starting from the optimal single elevation of 51°, just doubling the lights on a less optimal elevation, without adding a new azimuthal direction (blue curve), only slightly improves the outcome. With the same total number of lights, the optimal single elevation is superior. The twisted configuration (magenta) shows better results than the aligned configuration, but the error still lies above the optimal single elevation with the same number of lights. Seemingly, the inferiority of the second elevation angle outrivals its additional value to the solution.

4. Conclusions

The experiments made in Section 3.3 lead us to the following observations:

1. There is an optimal angle of elevation for incident light close to 51°.

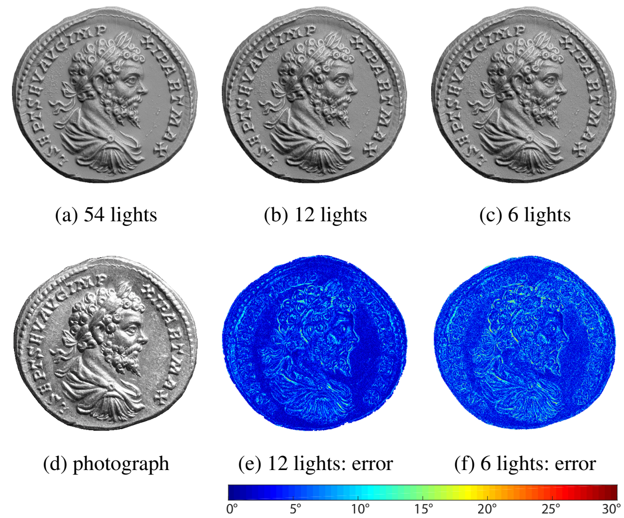

(a) 54 lights (b) 12 lights (c) 6 lights

(d) photograph (e) 12 lights: error (f) 6 lights: error

Figure 5: Example reconstruction of a Roman gold coin. Top row: renderings of reconstruction results using the whole light dome, as well as 12 and 6 lights at 51° of elevation. Bottom row: a photograph of the coin and visualizations of the angular errors.

2. Starting from a circular light arrangement at this angle, additional azimuths contribute more to the reconstruction than additional elevations.
3. Lights of additional azimuths contribute more to the reconstruction if they are located at the optimal elevation, than at another.

Therefore, a light dome could be fully replaced by a circular light arrangement for the problem of reconstructing historical coins without significant loss of quality. Figure 5 shows a qualitative result. Note that the 12- and 6-light reconstructions are visually not distinguishable from the full-dome reconstruction and high error values appear only locally on edges and cavities.

For future work, we plan to elaborate this study by applying optimal light configuration learning [LG14] and a quantitative comparison to structured light approaches.

Acknowledgements: The coins of this study have been kindly provided by the Museum of Fine Arts, Vienna, and the Museum Lauriacum, Enns.

References

[AG15] Ackermann J., Goesele M.: A Survey of Photometric Stereo Techniques. *Foundations and Trends in Computer Graphics and Vision 9*, 3-4 (2015), 149–254. 2, 3

[AMK07] Alldrin N. G., Mallick S. P., Kriegman D. J.: Resolving the generalized bas-relief ambiguity by entropy minimization. *Proc. CVPR* (2007), 1–7. 2

[ASSS14] Ahmad J., Sun J., Smith L., Smith M.: An improved photometric stereo through distance estimation and light vector optimization from diffused maxima region. *PRL 50* (2014), 15–22. 2

[AWL13] Aittala M., Weyrich T., Lehtinen J.: Practical SVBRDF capture in the frequency domain. *ACM Transactions on Graphics 32*, 4 (2013), 110. 2

[BKY99] Belhumeur P. N., Kriegman D. J., Yuille A. L.: The bas-relief ambiguity. *IJCV 35*, 1 (1999), 33–44. 2

[FSB04] Frolova D., Simakov D., Basri R.: Accuracy of Spherical Harmonic Approximations for Images of Lambertian Objects under Far and Near Lighting. *Proc. ECCV* (2004), 574–587. 2

[HW11] Herbort S., Wöhler C.: An introduction to image-based 3D surface reconstruction and a survey of photometric stereo methods. *3D Research 2*, 3 (2011), 1–17. 2

[HZKS13] Hödlmoser M., Zambanini S., Kampel M., Schlapke M.: Evaluation of historical coin 3d models. In *Proc. 38th Conf. on Comp. Applications and Quantitative Methods in Archaeology (CAA 2010)* (2013), pp. 499–504. 1

[JHMZF11] Jarrett J., Hüber-Mork R., Zambanini S., Felicetti A.: Coinage, digitization and the worldwide web: numismatis and the coins project. *New Technol. Mediev. Renaiss. Stud 3* (2011), 459–489. 1

[KGM] KHM coin collection. `https://www.khm.at/en/visit/collections/coin-collection/`. Accessed: 2018-07-18. 1

[LG14] Liu C., Gu J.: Discriminative illumination: Per-pixel classification of raw materials based on optimal projections of spectral BRDF. *IEEE PAMI 36*, 1 (2014), 86–98. 4

[LWYG07] Liao M., Wang L., Yang R., Gong M.: Light fall-off stereo. *Proc. CVPR* (2007), 1–8. 2

[MGW01] Malzbender T., Gelb D., Wolters H.: Polynomial texture maps. In *Proc. of the 28th Annual Conference on Computer Graphics and Interactive Techniques* (2001), ACM, pp. 519–528. 1

[MMH17] MacDonald L., Moitinho de Almeida V., Hess M.: Three-dimensional reconstruction of Roman coins from photometric image sets. *Journal of Electronic Imaging 26*, 1 (2017), 011017. 1

[MVSL05] Mudge M., Voutaz J.-P., Schroer C., Lum M.: Reflection transformation imaging and virtual representations of coins from the hospice of the grand st. bernard. In *Proc. 6th International Symposium on Virtual Reality, Archaeology and Cultural Heritage (VAST)* (2005), pp. 29–40. 1

[NIK90] Nayar S. K., Ikeuchi K., Kanade T.: Determining shape and reflectance of hybrid surfaces by photometric sampling. *IEEE Transactions on Robotics and Automation 6*, 4 (1990), 418–431. 2

[NRDR05] Nehab D., Rusinkiewicz S., Davis J., Ramamoorthi R.: Efficiently combining positions and normals for precise 3d geometry. *ACM Transactions on Graphics 24*, 3 (2005), 536–543. 1

[PF13] Papadhimitri T., Favaro P.: A new perspective on uncalibrated photometric stereo. *Proc. CVPR* (2013), 1474–1481. 2

[PSP*14] Palma G., Siotto E., Proesmans M., Baldassari M., Baracchini C., Batino S., Scopigno R.: Telling the story of ancient coins by means of interactive rti images visualization. *Proc. 40th Conf. on Comp. Applications and Quantitative Methods in Archaeology (CAA 2012),* (2014), 177–185. 1

[QLD15] Quéau Y., Lauze F., Durou J.-D.: Solving uncalibrated photometric stereo using total variation. *Journal of Mathematical Imaging and Vision 52*, 1 (2015), 87–107. 1, 2

[QMD16] Queau Y., Mecca R., Durou J.-D.: Unbiased Photometric Stereo for Colored Surfaces: A Variational Approach. *Proc. CVPR* (2016), 4359–4368. 2

[WGS*10] Wu L., Ganesh A., Shi B., Matsushita Y., Wang Y., Ma Y.: Robust photometric stereo via low-rank matrix completion and recovery. In *Proc. ACCV* (2010), Springer, pp. 703–717. 2

[Woo80] Woodham R. J.: Photometric Method For Determining Surface Orientation From Multiple Images. *Optical Engineering 19*, 1 (1980). 1, 2

[ZSKM09] Zambanini S., Schlapke M., Kampel M., Müller A.: Historical coins in 3d: acquisition and numismatic applications. In *Proc. 10th International Symposium on Virtual Reality, Archaeology and Cultural Heritage (VAST)* (2009), pp. 49–52. 1